Rapid Communications

Localization by virtual transitions in correlated disorder

Alex Dikopoltsev,[1,*] Hanan Herzig Sheinfux,[1,2] and Mordechai Segev[1]

[1]*Physics Department and Solid State Institute, Technion–Israel Institute of Technology, Haifa 32000, Israel*

[2]*ICFO-Institut de Cie´ncies Foto´niques, Mediterranean Technology Park, 08860 Castelldefels (Barcelona), Spain*

(Received 5 June 2019; revised manuscript received 3 September 2019; published 11 October 2019)

Anderson localization is fundamentally relevant to all physical systems where coherent waves evolve in the presence of disorder. Physically, any disorder must have a finite spectral bandwidth, hence the disorder is always correlated. Here, we study the regime of localization mediated by virtual transitions in correlated disorder. We find that wave packets centered outside of the spectral extent of the disorder can localize, with localization length almost as short as for localization via first-order transitions. In this regime, virtual transitions lead to phenomena with profound significance, such as mobility edges, and strong localization in regions of momentum space where otherwise localization would be extremely weak. Remarkably, in two-dimensional systems, we show localization can occur in directions that cannot be reached by direct scattering from the disordered potential.

DOI: 10.1103/PhysRevB.100.140202

Naively, random scattering is expected to produce diffusive transport. Yet coherent waves can behave differently: disorder can transform all the modes of the system into localized modes, bringing transport to a complete halt [1]. This discovery, known as Anderson localization, has become a cornerstone in the understanding of waves in random media. Over the years, localization has been studied in a variety of systems, ranging from light in scattering dielectric media [2,3] and in photonic lattices containing disorder [4,5] to sound waves [6], microwaves [7,8] and cold atoms [9–11], and has evolved into a rich field of research.

The hallmark of Anderson localization is that the eigenmodes of the system are exponentially localized, with localization length l_{loc}, which is the mean inverse decay rate of the modes. In infinite 1D or 2D disordered systems, all states are localized [12]. However, in systems of finite extent, some modes have localization length l_{loc} larger than the system size L, hence considered extended, whereas the modes with l_{loc} smaller than L are localized. Generally, the localization length depends on the strength of the disorder and on spatial correlations in the potential that are always present when the spectrum of the disorder has a finite extent.

To understand the effect of correlated disorder, it is instructive to consider localization from a spectral perspective. Consider first a 1D system with a disordered potential $V(x)$. The spatial power spectrum $|FT\{V(x)\}|^2$, which is also the Fourier transform (FT) of the two-point correlation function of the potential, $C_V(x,x')$, determines the range of possible scattering processes due to momentum exchange between the waves and the disorder [13–15]. Essentially, every spectral component of the disorder behaves as a diffraction grating that scatters one plane wave component into another.

In all of the above systems [2–11], the largest contribution comes from first-order (direct) transitions, where a single component from the spatial spectrum of the disordered potential is used during the scattering process [16]. The strength of localization, at a certain wave number $\vec{k}$, is characterized by a localization length $l_{\mathrm{loc}}(\vec{k})$ [17]. For first-order transitions, l_{loc} is inversely proportional to the FT of the correlation function at $\vec{k}$. These localized states possess a spatial spectrum that is strongly confined within the extent of the spectrum of the disordered potential. However, in a finite system the localization length can be much larger than the physical extent of the system, leading to modes that are effectively extended [8,13,18–20]. The cutoff between localized and extended states (for any finite systems in 1D or 2D) is referred to as the effective mobility edge [18,21–23], and it exists for all physical disordered systems.

It has been known for some time now that localization, as discovered by Anderson [1], is generally mediated by first-order (direct) transitions [16,17]. But, do first-order transitions describe all possible localization processes? In principle, second-order (virtual) transitions—mediated by two spectral components of the disorder—may also exist, but these are much less efficient than first-order ones [24] and are typically of negligible importance [9,22,23,25]. But what if first-order transitions are somehow forbidden and only second order ones are allowed?

Here we study Anderson localization induced by only second-order virtual transitions, second-order transitions with an intermediate virtual state, in correlated disordered. We find that the virtual transitions give rise to additional localized states at wave numbers much higher than the spectral cutoff, where localization should have otherwise been absent altogether. Likewise, we find that virtual transitions cause localization at low frequencies even when the spectrum of the disorder is completely shifted from zero. Specifically, we study the photonic scheme of transverse localization in disordered dielectrics, and find that, varying the incidence angle transforms the outcome from ballistic transport (as if the disorder was absent) to first-order localization, then again to a ballistic regime, followed by a regime of localization by solely second-order scattering. Finally, we explore 2D

*Corresponding author: alexdiko@technion.ac.il

spectrally shaped disordered potentials and show that they support localization at wave numbers where direct scattering from the disordered potential is impossible.

We follow the scheme of transverse localization [4,5,26,27], which is especially suitable for electromagnetic waves, where localization is manifested in arresting diffraction by multiple scattering from disorder. The system is described by

$$\frac{\partial A}{i\partial z} = \frac{1}{2k}\nabla_\perp^2 A + \frac{k}{n_0}\Delta n A, \tag{1}$$

where $A(\vec{r})$ is the slowly varying envelope of the field $E(\vec{r},t) = \mathrm{Re}[A(\vec{r})e^{i(kz-\omega t)}]$ with frequency ω and wave number $k = \omega n_0/c$, c is the vacuum light speed, n_0 and $\Delta n(x,y,z)$ are the ambient and the disordered local variation in the refractive index, respectively. Equation (1) is mathematically equivalent to the Schrödinger equation, where the z coordinate plays the role of the time, and $(-\Delta n/n_0)$ acts as the potential. Generally, for Anderson localization to occur the potential should be frozen in time, thus transverse localization requires that the random index change, Δn, would be z independent. Because Eq. (1) is linear, $\Delta n(x,y)$ can be written as a superposition of periodic functions, each acting as a grating component causing the spectral components of $A(\vec{r})$ to experience diffraction off this grating. Hence, localization may be viewed as an average over an ensemble of waves experiencing diffraction from randomly shifted gratings of multiple periodicities [16].

It is instructive to examine the system in momentum space. The evolution of a wave packet in k space is defined by the FT in the $x-y$ plane of Eq. (1)

$$\frac{\partial A_k}{i\partial z} = -\frac{1}{2k}k_\perp^2 A_k + \frac{k}{n_0}\Delta n_k * A_k, \tag{2}$$

where $A_k(k_x,k_y,z)$ and $\Delta n_k(k_x,k_y)$ are the 2D-FT of $A(x,y,z)$ and $\Delta n(x,y)$, with wave numbers k_x and k_y. Here, $k_\perp$ is the modulus of $\vec{k}_\perp = (k_x,k_y)$, and $*$ marks convolution. In the right-hand side of Eq. (2), when the contribution of the right (potential) term is much smaller than the left (kinetic) term, we can treat plane waves as eigenmodes of the system, coupled by convolutions with components in the spectrum of the disorder. These "transitions" in momentum space are naturally described by the coupled-mode formalism. The coupling between two different plane waves can occur if the potential contains a suitable disorder component that can momentum-match between the incident and scattered waves. Employing this coupled mode formalism is fully equivalent to solving Eq. (1) in real space, and therefore has analogies in other types of wave physics. It relies on phase-matched interactions, which in Eqs. (1) and (2) represent transitions that conserve momentum in z, while in the (analogous) Schrödinger equation such transitions are interpreted as energy conserving. A common example is a Laue equation governing x-ray diffraction, which states that for the diffraction condition to occur, it is required that $\mathbf{k}_{\mathrm{in}}\cdot\hat{\mathbf{K}} = |\mathbf{K}|/2$, $\mathbf{K}$ being the crystalline wave vector and $\mathbf{k}_{\mathrm{in}}$ is the incident wave. This is also known as the Bragg condition.

Consider first a simple example of a 1D correlated disorder. For concreteness, consider a 1D photonic structure with some random variation of the refractive index, $\Delta n(x)$, whose spatial FT, $\Delta n_k(k_x)$, consists of two regions in momentum space where the amplitude is uniform but the phase is random. Let us assume that spectral regions of the disorder are nonzero only in a small region Δk around some wave vector $k_0\hat{x}$ [Fig. 1(a)]. The two-point correlation function is $C_V(x,x') \propto \mathrm{FT}^{-1}\{|\Delta n_k|^2\} = \mathrm{sinc}((x-x')\Delta k)\cos(k_0(x-x'))$. For a plane wave incident upon this potential with wave number $k_{x,\mathrm{in}} \sim -k_0/2$, there are many possible phase-matched first-order transitions to the spectral region around $k_{x,1} \sim k_0/2$ [Fig. 1(b)], obeying $\Delta k_z(k_{x,\mathrm{in}}) = \Delta k_z(k_{x,1})$, where $\Delta k_z(k_x) = -{k_x}^2/2n_0k_0$. This plane wave undergoes many sequential first-order transitions, from positive to negative and back, leading to the buildup of Anderson localization [16].

However, our primary interest in this work is plane waves for which no phase matched first-order transitions exist; there are only second-order ones. Specifically, for a wave with spatial wave number $k_{x,\mathrm{in}} \sim -k_0$, the first-order transitions $-k_0 \xrightarrow{-k_0} -2k_0$ and $-k_0 \xrightarrow{+k_0} 0$ are not phase matched, but the second transition $0 \xrightarrow{k_0} k_0$, which makes the complete second-order transitions $-k_0 \xrightarrow{k_0} 0 \xrightarrow{k_0} k_0$, is matched [Fig. 1(b)]. We call the overall transition "virtual" because energy does not accumulate in the intermediate state at $k_x = 0$, similar to the role played by virtual levels in atomic systems. This transition requires two scattering events mediated by two spectral components (two random gratings), which may have the same or different wave numbers, as long as both have nonzero amplitudes, i.e., they are contained within the spectral extent of the disorder. For multiple scattering from disorder components with random phases, we expect the overall process to induce strong localization solely by virtual transitions, a phenomenon that was not yet observed in experiments.

To witness this effect, we first simulate the propagation dynamics of a Gaussian beam incident at various angles in a realistic photonic system with disorder in a 1D setting, described by the Δn_k in Fig. 2(a) and in further detail in the Supplemental Material [28]. The power spectrum of the disorder is concentrated in two narrow regions around k_0 and $-k_0$.

Figures 2(b)–2(f) show a top view of the wave propagating in this single realization of the disorder, for several angles of incidence. For some incidence angles there are no matched transitions and transport is nearly ballistic [e.g., Figs. 2(c) and 2(e)]. However, there are several ranges of incidence angles, for which transport is clearly localized. That is, they exhibit on-axis propagation, and do not expand in the transverse plane even after large distances—the hallmark of localization in the transverse localization scheme [4,26]. Physically, this is a consequence of scattering from the disorder, interfering destructively outside the center of the wave packet.

Localized behavior, i.e., on-axis propagation at zero transverse velocity without spatial expansion, is seen in Figs. 2(b), 2(d), and 2(f). In Fig. 2(d), for $k_{\mathrm{in}} = k_0/2$, localization is due to first-order transitions, which are phase-matched. However, the localization seen in Fig. 2(b) for $k_{\mathrm{in}} = 0$ and in Fig. 2(f) for $k_{\mathrm{in}} = k_0$ is due to second-order virtual transitions (involving an intermediate virtual state). For $k_{\mathrm{in}} = 0$ the overall virtual transitions are $0 \xrightarrow{k_0} k_0 \xrightarrow{-k_0} 0$ and $0 \xrightarrow{-k_0} -k_0 \xrightarrow{k_0} 0$, both are

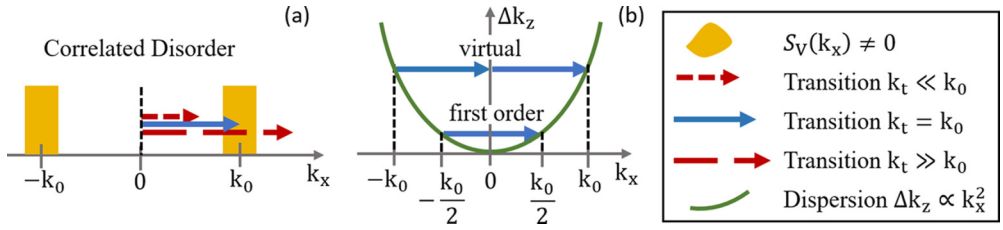

FIG. 1. Scattering transitions in momentum space. (a) Power spectrum $S_V(k_x)$ of a 1D disordered potential concentrated in two finite bands. The arrows represent transitions in k space, k_t. The blue arrow represents a possible scattering process mediated by a spectral component with $k_t = k_0\hat{x}$. The red arrows show transitions that are not supported by this potential. (b) Examples of scattering processes mediated by the $k_0\hat{x}$ spectral component of the disorder (blue arrow). The green curve is the phase mismatch $|\Delta k_z(k_x)| = k_x^2/2n_0k$. First-order phase-matched transition: a wave of wave number $-k_0/2$ scatters into a wave at $k_0/2$, so that $\Delta k_z(-k_0/2) = \Delta k_z(k_0/2)$. Second-order phase-matched transition: first, a wave scatters from $-k_0$ to a wave at $k_x = 0$. This transition alone is not efficient due to high phase mismatch. However, a subsequent second transition from $k_x = 0$ to a wave at k_0 makes the overall transition efficient, which eventually leads to localization by second-order virtual transitions. The intermediate state at $k_x = 0$ is called "virtual" because it cannot be reached by a single phase-matched scattering event in this scheme.

phase-matched, while for $k_{in} = k_0$ the transitions are $-k_0 \xrightarrow{k_0} 0 \xrightarrow{k_0} k_0$ and back $k_0 \xrightarrow{-k_0} 0 \xrightarrow{-k_0} -k_0$ around $k = 0$.

For all localized beams, the wave packet initially expands, but after some distance the expansion stops, in accordance with the evolution of the spatial spectrum [29]. The width of the beam, corresponding to the localization length, is best characterized by examining an ensemble average over many realizations of the disorder [4]. Hence, Fig. 2(g) shows the calculated effective width of the wave packet, $w_{eff} = \langle P \rangle^{-1}$, where $P = [\int I^2(x, L)dx]/[\int I(x, L)dx]^2$ is the inverse participation ratio, for an ensemble average over 100 realizations of disorder with power spectra in the region defined in Fig. 2(a). As marked by the red line in Fig. 2(g), the beam incident at $k_0/2 < k_{in} < k_0$ expands linearly as an undisturbed Gaussian beam. On the other hand, as highlighted by the blue line in Fig. 2(g), at $k_{in} = k_0/2$ the wave packet initially expands slightly and then its effective width becomes constant, i.e., the wave packet has become localized by first-order processes.

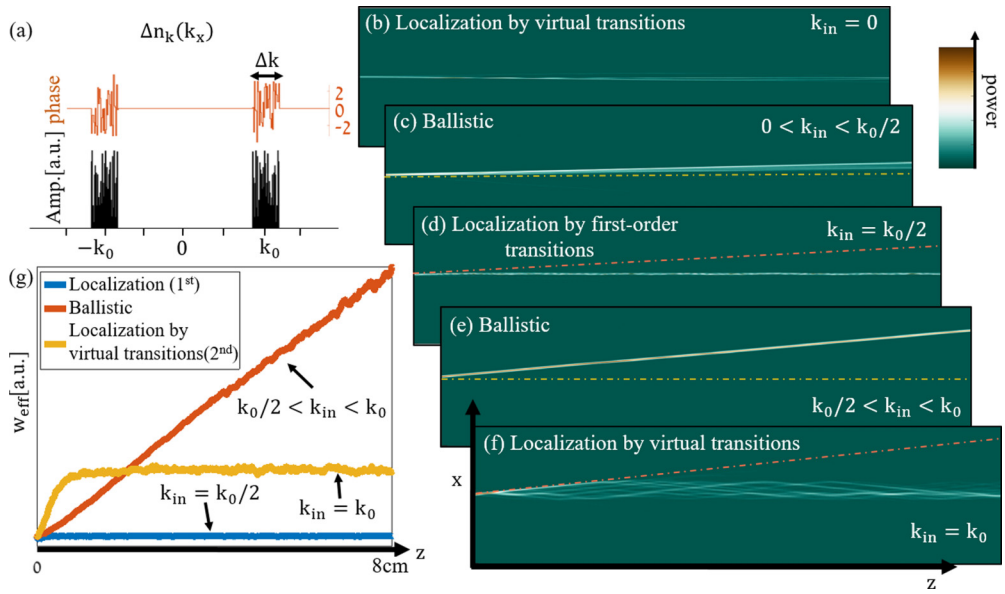

FIG. 2. Simulations of beam propagation and localization in correlated disorder. (a) Power spectrum of disorder concentrated in two narrow regions Δk around wave numbers k_0 and $-k_0$. (b)–(f) Simulated propagation of an initially Gaussian beam launched at various incidence angles corresponding to different k_{in} values. The dashed-dotted yellow line marks the $x = 0$ line, while the dashed-dotted orange line marks the propagation direction in the absence of disorder (homogeneous medium). (b) At $k_{in} = 0$ the beam propagates on the z axis without expanding due to a second-order process. (c) At $0 < k_{in} < k_0/2$, the transitions are phase mismatched, so the beam propagates ballistically, unaffected by the disorder. (d) For $k_{in} = k_0/2$, multiple first-order transitions are phase matched, hence the beam is localized and exhibits on-axis propagation (e) $k_0/2 < k_{new} < k_0$, same as (c): the beam evolves ballistically on its initial trajectory, unaffected by the disorder. (f) Evolution in the regime of localization by virtual transitions. Initially, the wave packet expands but after some distance the expansion stops. (g) Effective width w_{eff} as a function of propagation distance, representing an ensemble average over 100 realizations of disorder with a power spectrum as in (a). The beam incident at $k_0/2 < k_{in} < k_0$ expands linearly as an undisturbed Gaussian beam. At $k_{in} = k_0/2$ the wave packet initially expands slightly and then its w_{eff} becomes constant as the beam localizes. At $k_{in} = k_0$, the beam experiences intense expansion, but after some distance it eventually becomes localized, marking localization by virtual transitions.

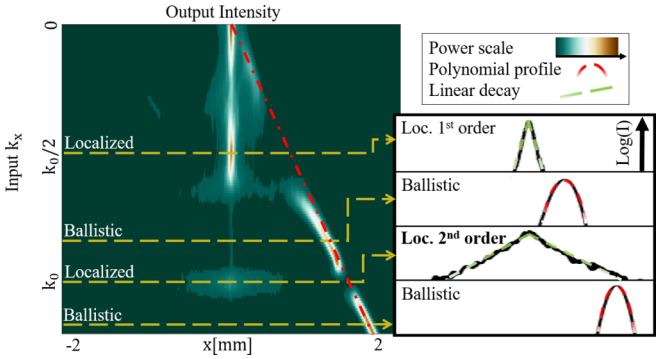

FIG. 3. Left: Ensemble average of the output intensity distribution for various input wave numbers, k_{in}. Right: beam cross sections for input wave numbers for which first-order and second-order localization occur, with the ballistic regimes in between. At $k_0/2$, the beam is localized by first-order phase-matched transitions, but localization occurs also at k_0, induced by virtual transitions only. At other incidence angles the wave packet stays Gaussian (polynomial in the log-scale). The centers of output beams that would have propagated in the same system, but with a homogenous refractive index, are marked with a red dashed line.

Curiously, we observe that at $k_{\text{in}} = k_0$, which is completely outside the immediate extent of the potential, the beam is also localized [yellow line in Fig. 2(g)], although at a broader cross section than in the "natural" localization regime by first-order transitions. This is the regime of localization by second-order virtual transitions. The effective width of the ensemble average beam first undergoes expansion, but after this initial expansion the beam becomes localized.

Next, we examine the cross-section of the evolving ensemble-average beams. Figure 3 shows the ensemble-average beam profile after propagating 26mm, for the incidence angle range $0 \leqslant k_{\text{in}} \leqslant 1.2k_0$. Here, for example, if a beam is incident at $x = 0$ and $k_{x,\text{in}} \sim k_0$, and propagates ballistically in a homogenous medium, the output beam will follow its initial trajectory and will be centered around $x = 1.7$ mm. The centers of output beams that would have propagated in this system but with a homogenous refractive index are marked with a red dashed line. The ensemble average beam displays a log-linear (exponential) decay at both $k_{\text{in}} = k_0/2 \equiv k_{\text{loc}}$ and at $k_{\text{in}} = k_0$, the hallmark of Anderson localization. At other angles, the wave packet remains Gaussian, expressed as a polynomial in the log-scale.

Having found localization by virtual transitions for an initially incident Gaussian beam at $k_{\text{in}} = k_0$, we proceed to calculate the localized modes. We calculate these in the presence of the same correlated disorder used for Figs. 2 and 3 (modes shown in the Supplemental Material), and compare it to disorder with a finite uniform spectrum. Figure 4 shows w_{eff} for various strengths of disorder (Δn) and system sizes L, for two types of disorder: one with an upper cutoff in the power spectrum at $2k_{\text{loc}} = k_0$ [Fig. 4(a)], and another with a narrow power spectrum around k_0 [Fig. 4(b)]. The horizontal axis corresponds to the central momentum of the mode, defined as $k_{x,c} = |\sqrt{k^2n^2 - \beta^2}|$, where β is the propagation constant of the mode. It is clear that the lower limit of w_{eff} is mainly defined by the power spectrum at specific wave numbers, hence l_c sets the minimum value of w_{eff}, while the upper limit is set by the system size L. Figures 4(a) and 4(b) show first-order localization with short l_c, below and in the vicinity of k_{loc}, respectively. However, Fig. 4(b) also presents second-order localization at $2k_{\text{loc}}$, induced by virtual transitions, with relatively small l_c (compared to L). Likewise, Fig. 4(b) displays second-order localization at 0. In fact, Fig. 4(b) shows mobility edges that, to our knowledge, have never been observed: one mobility edge slightly above $k_{\text{in}} = 0$ and two more mobility edges near $2k_{\text{loc}} - \Delta k/2$ and $2k_{\text{loc}} + \Delta k/2$. These effective mobility edges arise (in our system of finite width L) when the disorder becomes strong enough, causing all transport to stop above (or below, according to the edge position) certain wave numbers, when l_c becomes smaller than L.

Finally, we study second-order localization under 2D correlated disorder. To date, correlated disorder in systems with a finite spectrum was studied for radially symmetric spectra [20] or for trivially anisotropic spectra [30,31], where localization mediated by high-order was not shown. In 2D potentials, the localization length is expected to be very sensitive to the incidence angle. Specifically, disorder components can mediate transitions (of any order) only on a

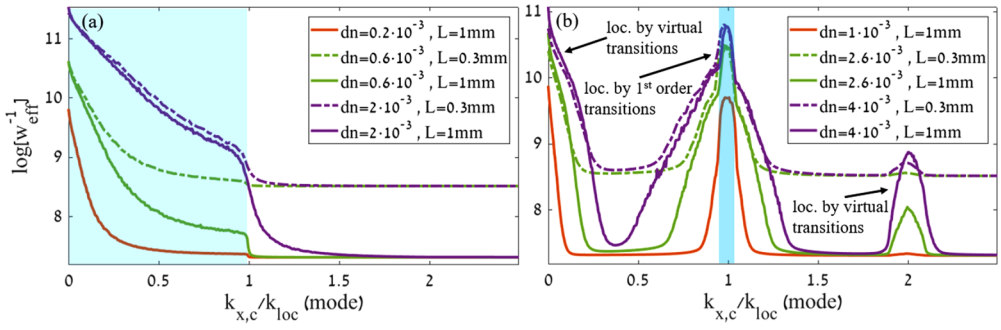

FIG. 4. Effective beam width w_{eff} for two types of correlated disorder: (a) when the disorder spectrum has a cutoff frequency at $2k_{\text{loc}}$, and (b) when the disorder spectrum has two narrow spectral bands around $2k_{\text{loc}}$, shifted from zero. The blue region marks the spectral extent of the disorder for each type ($2k_{\text{loc}}$ in the spectrum corresponds to k_{loc} in the spectral extent). The plots in (a) and (b) are calculated for various strengths of disorder (Δn) and system sizes L. The upper bound on the inverse effective width is mainly defined by l_c (determined by the strength of the disorder at specific wave numbers), while the lower bound is set by L. (b) Localization of the first-order with short l_c, in the vicinity of $k_{\text{loc}} \equiv k_0/2$ and localization induced by virtual transitions at $2k_{\text{loc}}$ and at 0 with an l_c relatively small compared to L.

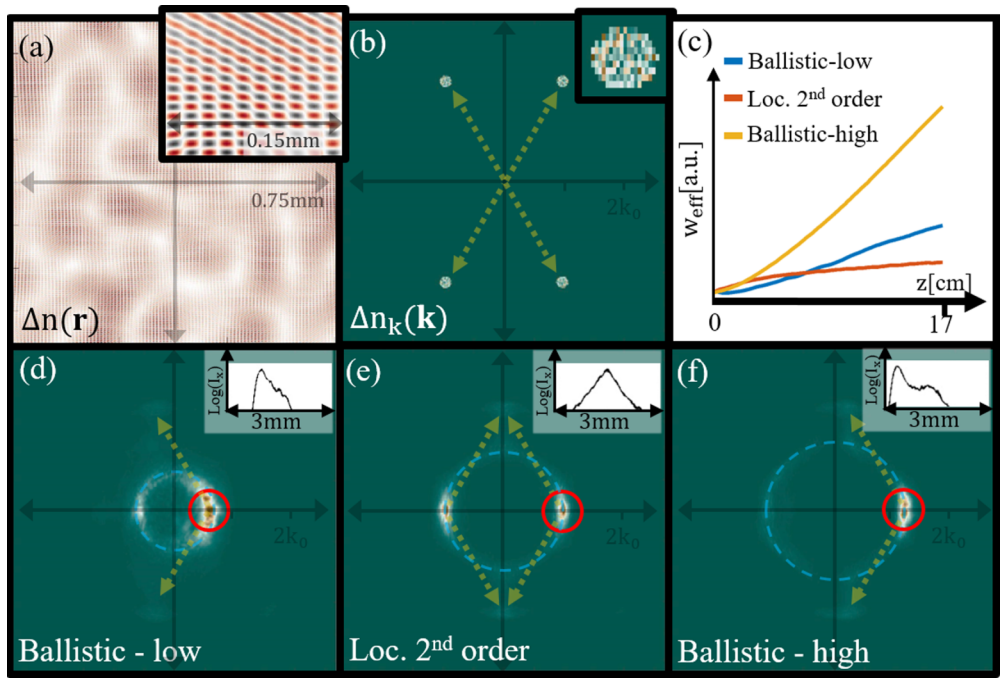

FIG. 5. Localization on the x axis strictly by virtual transitions in 2D correlated disorder. (a),(b) Example of a disordered potential $\Delta n(x, y)$ whose FT is the spectrum in (b). The features consist of small scale and large scale structures (enlarged in the inset). The spectrum consists of finite regions of random coefficients located symmetrically on the vertices of a rectangle in k space with size $[-k_0, k_0] \times [-\sqrt{3}k_0, \sqrt{3}k_0]$. Yellow arrows mark possible transitions. (c) Effective beam width w_{eff}, for 20 disorder realizations, for incidence angles: at (red), below (blue) and above (yellow) the angle associated with localization by virtual transitions. (d),(e),(f) Spectra of beams after 10 cm of propagation, (e) the angle where second-order virtual transitions are phase matched, (d),(f) lower and higher incidence angle, where both first and second-order transitions are phase mismatched. Red circles mark the central wave number at incidence and blue dashed circles mark the phase-matched k. Insets: intensity cross section in the x direction of the ensemble-averaged beam for 100 realizations of disorder in log scale for the three angles [inset (e) shows exponential decay, while (d) and (f) stay mainly Gaussian].

phase-matched circle of radius $|\mathbf{k}_{\text{in}}|$, and localization will occur around the symmetry axis of the overall transition. Having phase-matched second-order transitions allows localization to occur in different spectral regions, which otherwise would not occur. Here, we choose a disordered potential that has roughly rectangular symmetry in k space [Fig. 5(a)]. We create the 2D disorder by defining nonzero Fourier coefficients in small regions located on vertices of a rectangle with size $[-k_0, k_0] \times [-\sqrt{3}k_0, \sqrt{3}k_0]$ [Fig. 5(b)]. We simulate the propagation of a 2D Gaussian beam with spectral width approximately half of the width of the k-space regions of the disorder, launched at different incidence angles, corresponding to $\mathbf{k}_{\text{in}} = k_0(0.6, 0)$, $k_0(1, 0)$ and $k_0(1.2, 0)$. Figure 5(c) shows the effective width of these 2D beams. We find that for $\mathbf{k}_{\text{in}} = k_0(1, 0)$, the second-order transitions are phase matched and allow for localization in the direction of the x-axis [Fig. 5(e)], a direction for which first-order localization does not exist whatsoever. That is, the spectrum of the disorder does not support first-order transitions that would lead to localization in the x direction, yet this system does exhibit localization strictly by second-order scattering processes via virtual states. Moreover, as shown here, transitions at intermediate angles, such as $\mathbf{k}_{\text{in}} = k_0(0.6, 0)$ or $k_0(1.2, 0)$, are not phase matched, hence cannot induce localization; instead the beam incident at these angles experiences ballistic-like propagation [Figs. 5(d) and 5(f)]. Clearly, for beams launched at $\mathbf{k}_{\text{in}} = k_0(1, 0)$, where phase-matched second-order virtual transitions are allowed, diffraction is arrested [Fig. 5(c)], while beams launched at the other angles experience ballistic transport (w_{eff} proportional to z). We find that virtual transitions bring the beam expansion to a halt, the hallmark of localization. The insets in Figs. 5(d), 5(e), and 5(f) show the cross section of the ensemble-averaged beam for 100 realizations of the disorder: Fig. 5(e) is linearly decaying in log scale, meaning it is exponentially localized, while Figs. 5(d) and 5(f) display roughly a Gaussian shape.

Examining the scattering processes of coherent wave packets in systems containing disorder of a finite spectral extent led us to find localization caused solely by virtual transitions. We have shown that the outcome is indeed Anderson localization, with exponentially decaying tails. This type of localization, induced by second-order phase-matched transitions, exists in any system at least for zero momentum (e.g., amorphous structures with an effective gap [32,33] or high-density hyperuniform materials [31]), and is therefore observable in experiments. Definitely, localization induced by third-order transitions or higher is also possible, but the localization length increases with increasing order, and might extend beyond the scale of the system. Interestingly, we have shown that already second-order transitions can cause localization in directions that are not directly supported by the disordered potential. Altogether, it is now clear that, although Anderson localization is a linear phenomenon, the processes involve deep physics that offers new surprises even 60 years after it was originally discovered.

The authors wish to thank Prof. B. Shapiro (Technion) and Prof. Y. Bar Lev (Ben Gurion University) for useful discussions. This research was supported by the Israel Science Foundation and by the German-Israeli DIP Program. H.H.S. gratefully acknowledges the support by a Marie Skłodowska-Curie fellowship.

[1] P. W. Anderson, Phys. Rev. **109**, 1492 (1958).
[2] D. S. Wiersma, P. Bartolini, A. Lagendijk, and R. Righini, Nature (London) **390**, 671 (1997).
[3] M. Störzer, P. Gross, C. M. Aegerter, and G. Maret, Phys. Rev. Lett. **96**, 063904 (2006).
[4] T. Schwartz, G. Bartal, S. Fishman, and M. Segev, Nature (London) **446**, 52 (2007).
[5] Y. Lahini, A. Avidan, F. Pozzi, M. Sorel, R. Morandotti, D. N. Christodoulides, and Y. Silberberg, Phys. Rev. Lett. **100**, 013906 (2008).
[6] H. Hu, A. Strybulevych, J. H. Page, S. E. Skipetrov, and B. A. van Tiggelen, Nat. Phys. **4**, 945 (2008).
[7] A. A. Chabanov, M. Stoytchev, and A. Z. Genack, Nature **404**, 850 (2000).
[8] U. Kuhl, F. M. Izrailev, A. A. Krokhin, and H. J. Stöckmann, Appl. Phys. Lett. **77**, 633 (2000).
[9] J. Billy, V. Josse, Z. Zuo, A. Bernard, B. Hambrecht, P. Lugan, D. Clément, L. Sanchez-Palencia, P. Bouyer, and A. Aspect, Nature (London) **453**, 891 (2008).
[10] S. S. Kondov, W. R. McGehee, J. J. Zirbel, and B. DeMarco, Science **334**, 66 (2011).
[11] F. Jendrzejewski, A. Bernard, K. Müller, P. Cheinet, V. Josse, M. Piraud, L. Pezzé, L. Sanchez-Palencia, A. Aspect, and P. Bouyer, Nat. Phys. **8**, 398 (2012).
[12] E. Abrahams, P. W. Anderson, D. C. Licciardello, and T. V. Ramakrishnan, Phys. Rev. Lett. **42**, 673 (1979).
[13] S. John and M. J. Stephen, Phys. Rev. B **28**, 6358 (1983).
[14] D. H. Dunlap, H. L. Wu, and P. W. Phillips, Phys. Rev. Lett. **65**, 88 (1990).
[15] J. C. Flores, J. Phys. Condens. Matter **1**, 8471 (1989).
[16] G. Samelsohn, S. A. Gredeskul, and R. Mazar, Phys. Rev. E **60**, 6081 (1999).
[17] I. M. Lifshits, S. A. Gredeskul, and L. A. Pastur, *Introduction to the Theory of Disordered Systems* (Wiley-Interscience, 1988).
[18] F. M. Izrailev and A. A. Krokhin, Phys. Rev. Lett. **82**, 4062 (1999).
[19] V. Bellani, E. Diez, R. Hey, L. Toni, L. Tarricone, G. B. Parravicini, F. Domínguez-Adame, and R. Gómez-Alcalá, Phys. Rev. Lett. **82**, 2159 (1999).
[20] M. Piraud, A. Aspect, and L. Sanchez-Palencia, Phys. Rev. A **85**, 063611 (2012).
[21] S. John, Phys. Rev. Lett. **58**, 2486 (1987).
[22] P. Lugan, A. Aspect, L. Sanchez-Palencia, D. Delande, B. Grémaud, C. A. Müller, and C. Miniatura, Phys. Rev. A **80**, 023605 (2009).
[23] E. Gurevich and O. Kenneth, Phys. Rev. A **79**, 063617 (2009).
[24] L. Tessieri, J. Phys. A. Math. Gen. **35**, 9585 (2002).
[25] L. Sanchez-Palencia, D. Clément, P. Lugan, P. Bouyer, G. V. Shlyapnikov, and A. Aspect, Phys. Rev. Lett. **98**, 210401 (2007).
[26] H. De Raedt, A. Lagendijk, and P. de Vries, Phys. Rev. Lett. **62**, 47 (1989).
[27] M. Segev, Y. Silberberg, and D. N. Christodoulides, Nat. Photonics **7**, 197 (2013).
[28] See Supplemental Material at http://link.aps.org/supplemental/10.1103/PhysRevB.100.140202 for simulation details and calculated eigenmodes in correlated disorder.
[29] L. Levi, M. Rechtsman, B. Freedman, T. Schwartz, O. Manela, and M. Segev, Science **332**, 1541 (2011).
[30] M. Piraud, L. Pezze, and L. Sanchez-Palencia, New J. Phys. **15**, 075007 (2013).
[31] O. Leseur, R. Pierrat, and R. Carminati, Optica **3**, 763 (2016).
[32] C. Jin, X. Meng, B. Cheng, Z. Li, and D. Zhang, Phys. Rev. B **63**, 195107 (2001).
[33] M. Rechtsman, A. Szameit, F. Dreisow, M. Heinrich, R. Keil, S. Nolte, and M. Segev, Phys. Rev. Lett. **106**, 193904 (2011).